ACS APPLIED MATERIALS & INTERFACES

Research Article

www.acsami.org

Elucidating the Crucial Role of Hole Injection Layer in Degradation of Organic Light-Emitting Diodes

Tae-Hee Han,[†] Wonjun Song,[‡] and Tae-Woo Lee*[,†]

[†]Department of Materials Science and Engineering, Pohang University of Science and Technology (POSTECH), Pohang, Gyungbuk 790-784, Republic of Korea

[‡]Samsung Display Co., Ltd., 95 Samsung 2-ro, Giheung-gu, Yongin-city, Gyeonggi-Do 446-711, Republic of Korea

Supporting Information

ABSTRACT: Although the luminous efficiency has been significantly improved in multilayered organic light-emitting diodes (OLEDs), understanding the major factors that influence degradation of OLEDs remains a major challenge due to their complex device structure. In this regard, we elucidate the crucial role of hole injection layer (HIL) in degradation of OLEDs by using systematically controlled hole injection interfaces. To analyze charge injection dependent degradation mechanism of OLEDs, we fabricate multilayered small-molecule OLEDs with molecularly controlled HILs. Although a reduced hole injection energy barrier greatly improves both a luminous efficiency and an operational lifetime (>10 times) of the OLEDs at the same time, large hole injection energy barrier increasingly aggravates its charge injection and transport during device operation. By using various kinds of nondestructive analyses at gradual stages of degradation, we demonstrate that accumulated charges at interfaces due to inefficient charge injection accelerates rate of device degradation.

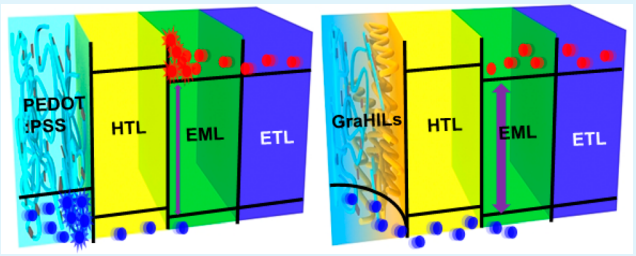

KEYWORDS: *organic light-emitting diodes, degradation, device stability, hole injection interface*

INTRODUCTION

Organic light-emitting diodes (OLEDs) have been considered as a promising candidate for environmentally sustainable and energetically efficient next-generation displays and solid-state lighting.[1−8] However, the electrical and luminescent properties of OLEDs are rapidly degraded at high luminance, and this problem must be overcome. Therefore, to develop stable devices with long lifetime, the mechanism that causes operational degradation of OLEDs must be understood.[9−11] Several complex factors are involved in degradation of small-molecule based OLEDs. To confine free charge carriers, small-molecule-based OLEDs are usually composed of several functional layers such as injecting and transporting layers so that they include several interfaces between layers.[11−15] To obtain OLEDs with high stability, the energy barrier between anode and emitting layer (EML) must be small and inserting hole transporting layers (HTLs) with adaquate ionization potential (IP) between the anode and the EML can reduce the hole injection barrier.[10,16]

In this study, we focused on the effect of the hole-injecting interface between indium−tin-oxide (ITO) anode and HTL on the device efficiency and lifetime by controlling the molecular interfaces of hole-injection layers (HILs). A conducting polymer, poly(3,4-ethylenedioxythiophene):poly-(styrenesulfonate) (PEDOT:PSS), has been widely used as the HIL in OLEDs, but the low IP of PEDOT:PSS (~5.0−5.2 eV) forms a hole injection energy barrier at the interface between the HIL and EMLs or HTLs (IP ≥ 5.4 eV). Furthermore, the insufficient electron and exciton quenching blocking capability of PEDOT:PSS limits the luminous efficiency and stability of OLEDs.[17,18] We used a HIL composed of PEDOT:PSS and tetrafluoroethylene−perfluoro-3,6-dioxa-4-methyl-7-octenesulfonic acid copolymer, a perfluorinated ionomer (PFI). Various ratios of PFI to PEDOT:PSS provides a variety of molecularly controlled interfaces between the HIL and the HTL. PFI has a lower surface energy than does PEDOT:PSS, so a mixture of the two substances are self-organized; the concentration of PFI chains is gradually increased from the bottom to the top surface of the film (Supporting Information, Figure S2). Furthermore, PFI has a higher ionization potential than does PEDOT:PSS, so the top surface of the gradient HIL (GraHIL) film thus formed has a much higher ionization potential than does PEDOT:PSS.[18−21] The surface work function (WF) of a GraHIL can be adjusted by controlling the proportion of PFI in the compositions (PEDOT:PSS, ~5.2 eV; GraHIL21, ~5.8 eV) (Supporting Information, Table S1). The gradient WF of GraHILs enables holes to be easily injected into the HTL and the EML. Furthermore, the PFI rich surface is insulating so that it effectively blocks electrons and excitons, thus confining carriers and achieving efficient radiative recombination of excitons in the EML.[18] Additionally, self-organized PFI layers

Received: October 20, 2014
Accepted: January 6, 2015
Published: January 6, 2015

DOI: 10.1021/am5072628
ACS Appl. Mater. Interfaces 2015, 7, 3117−3125

can block metal atoms that diffused out from the ITO anode due to etching by acidic PEDOT:PSS.[19,22,23] In general, metal atoms such as In and Sn degrade device performance by trapping carriers and by metal induced nonradiative recombination of excitons.[21−23] To analyze the processes of device degradation with various hole-injecting interfaces, we performed current−voltage−luminance (I−V−L), operational lifetime, capacitance−voltage (C−V), transient electroluminescence (EL), steady-state EL, photoluminescence (PL) measurements, and Raman spectroscopy to systematically characterize devices at various degraded stages.

EXPERIMENTAL SECTION

OLED Fabrication. Glass coated with Indium−tin-oxide (ITO; WF ∼4.8 eV) (square active areas: 2 × 2 mm) were used as substrates and anodes. Ultraviolet ozone treatment was applied to cleaned ITO surface for 15 min before spin-coating of polymeric HIL films on top of it. Various GraHILs were composed of PEDOT:PSS (CleviosTM P VP AI4083) and a tetrafluoroethylene-perfluoro-3,6-dioxa-4-methyl-7-octene-sulfonic acid copolymer (CAS number: 31175-20-9) (Sigma-Aldrich Inc.). We adjusted surface work function (WF) of the HIL by controlling the relative concentration of PFI to PEDOT:PSS in GraHIL compositions. (weight ratio of PEDOT/PSS/PFI and surface WF: GraHIL21 (1/6/12.7) ∼ 5.79 eV, GraHIL41 (1/6/6.3) ∼ 5.72 eV, GraHIL81 (1/6/3.2) ∼ 5.63 eV, PEDOT:PSS (1/6/0) ∼ 5.20 eV) (Supporting Information, Table S1) Various GraHIL polymer compositions were deposited as 50 nm films by spin-coating, then immediately baked on a hot plate at 200 °C for 10 min in ambient atmosphere. Small molecules such as N,N′-bis(inaphthyl)-*N*,*N*′-diphenyl-1,1′-biphenyl-4,4′-diamine (NPB) as the hole transport layer (HTL), bis(10-hydroxybenzo[*h*]quinolinato) beryllium ($Bebq_2$) as the electron transport layer (ETL) or the host material for the emitting layer (EML) and a green-light-emitting fluorescent material C545T (2% codeposition with $Bebq_2$) as the dopant material were sequentially deposited in sequences and thicknesses appropriate for the intended device structure by thermal evaporation. Then lithium fluoride (1 nm) and aluminum (130 nm) layers were sequentially deposited on the ETL as the cathode. All thermal evaporation was conducted under ultrahigh vacuum (<5 × 10^{-7} Torr). All fabricated devices were sealed by glass encapsulation using a UV resin with a getter.

OLED Characterizations. To measure current−voltage−luminance (I−V−L) characteristics and EL spectra, a source-measurement unit (Keithley 236) and a spectroradiometer (Minolta CS2000) were used. The steady-state photoluminescence (PL) spectra of devices were measured by using a PL spectrometer (JASCO FP6500) with a excitation wavelength at 415 nm. Capacitance−voltage characterizations of devices were conducted with electrochemical impedance spectroscopy (Bio-logic SP-300). All the devices were biased from 0 to 4 V at constant frequency, 1000 Hz, in the dark. For transient EL measurement, constant electrical pulse (100 s width and 10 Hz frequency) was applied to devices by using a pulse generator (HP 8116A). The emitted light is detected by using a photon-counting-spectrofluorometer (ISS PC1), and EL rising output signal was measured by an oscilloscope (Agilent infiniium 54832B DSO).

RESULTS AND DISCUSSION

Hole Injection. To prove the superior hole-injecting capability of our GraHILs, we fabricated hole-only devices [ITO/HIL (50 nm)/NPB (300 nm)/Al (150 nm)] using GraHILs with various ratios of PFI to PEDOT:PSS (GraHIL21 (∼5.8 eV), GraHIL41 (∼5.7 eV) and GraHIL81(∼5.6 eV)), and a general PEDOT:PSS (∼5.2 eV)) (Figure 1a). Hole-only devices with GraHILs exhibited much higher current densities than did the device with the PEDOT:PSS (Figure 1b). The gradient and high surface WF of GraHILs reduced the hole-injection energy barrier between ITO (∼4.7−4.9 eV) and HTL

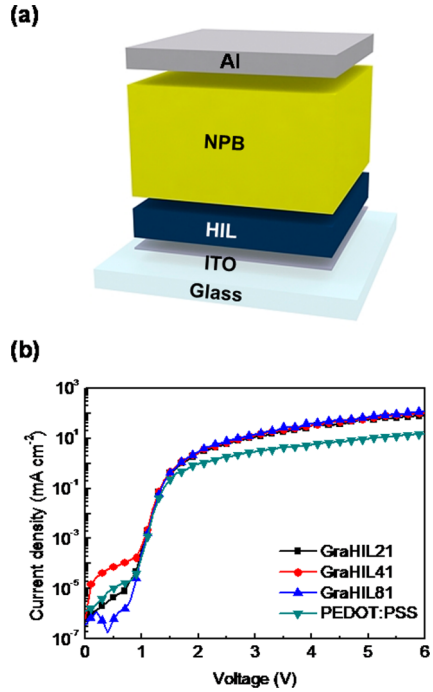

Figure 1. (a) Schematic illustration of hole-only devices with various HILs, (b) Hole current densities of hole-only devices (HIL: GraHIL21, GraHIL41, GraHIL81 or PEDOT:PSS).

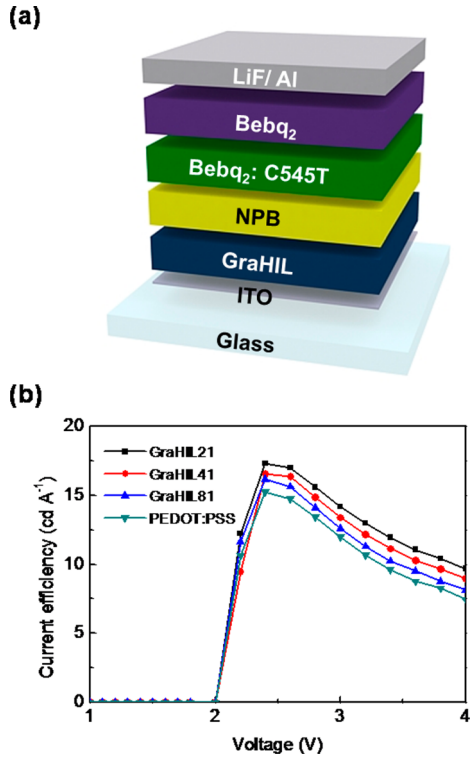

Figure 2. (a) Schematic illustration of multilayered, fluorescent green OLED based on small-moleule. (b) Current efficiency versus voltage characteristics of fluorescent green OLEDs using GraHIL21, GraHIL41, GraHIL81 or PEDOT:PSS.

(i.e., NPB ∼5.4 eV). Because GraHILs provide highly efficient hole injection, they can inject holes into the HTL and the EML more easily than can PEDOT:PSS. We also fabricated green fluorescent small-molecule OLEDs [ITO/HIL (50 nm)/NPB

DOI: 10.1021/am5072628
ACS Appl. Mater. Interfaces 2015, 7, 3117−3125

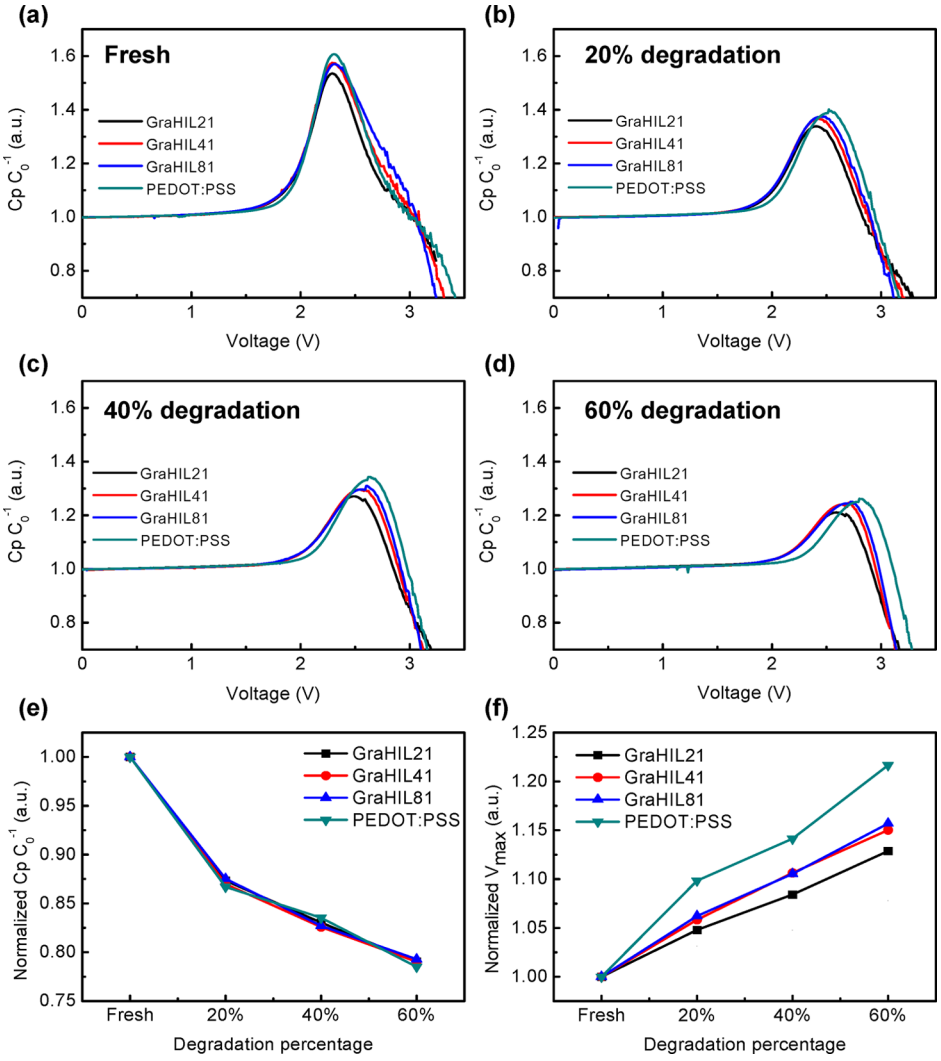

Figure 3. Capacitance versus voltage characteristics of OLEDs using GraHIL21, GraHIL41, GraHIL81 or PEDOT:PSS. Normalized capacitance (C_p C_0^{-1}) versus voltage curves of devices at (a) fresh (0%), (b) 20%, (c) 40% and (d) 60% degraded stages of initial luminance under constant current operation. Changes of (e) normalized peak capacitance (C_p C_0^{-1}) and (f) voltage at the peak capacitance (V_{max}) under device degradation.

(20 nm)/$Bebq_2$:C545T (2%, 30 nm)/$Bebq_2$ (20 nm)/LiF (1 nm)/Al (150 nm)] with GraHILs or PEDOT:PSS as the HIL (Figure 2a). Increasing the PFI concentration in PEDOT:PSS caused the current efficiency (CE) to increase, due to improved hole injection from the ITO anode to HTL and to blocking of electrons by the self-organized PFI layer, which thus confines the carriers and achieves efficient recombination of electrons and holes in the EML. Green fluorescent OLEDs with GraHILs exhibited gradually enhanced CEs (max. CE with GraHIL21 ~ 17.3 cd A^{-1}, GraHIL41 ~ 16.5 cd A^{-1}, GraHIL81 ~ 16.2 cd A^{-1}) compared to that with general PEDOT:PSS HIL (~15.2 cd A^{-1}) (Figure 2b).

Capacitance–Voltage Characteristics. We also performed many kinds of nondestructive analyses of green fluorescent small-molecule OLEDs at four degradation stages (fresh, 20%, 40% and 60% degraded) respectively. To investigate the influence of device operation on charge-injecting and -transporting properties of OLEDs, we conducted C–V characterizations in devices with various HILs (Figure 3). The C–V characteristics can provide information regarding the injection regime of charge carriers. A sharp increase of capacitance from the geometric capacitance (C_0) in the dark current regime due to movement of intrinsic charge carriers in the organic films means that majority carriers are being injected. When minority carriers are injected into the EML, a sharp decline of capacitance is observed due to recombination of majority and minority carriers at the turn-on voltage (V_{to}).[24] The LiF/Al cathode is widely used to reduce the effective WF of Al cathode and to enhance electron injection. The effectiveness with which the LiF layer lowers the WF of Al (<3 eV) suggests that ohmic contact is formed between the cathode and the organic ETL ($Bebq_2$).[25−27] In addition, our EML of OLEDs includes an electron-transporting host ($Bebq_2$) that has high electron mobility (~10^{-4} cm^2/V s) and low hole mobility (~10^{-6} cm^2/V s).[28] Therefore, in the EML, electrons are more mobile than holes because of nearly ohmic electron injection without an energy barrier from the cathode and because of electron-dominant device architecture. In contrast, the hole-injection interface at PEDOT:PSS/NPB shows a low hole injection efficiency (~0.2) calculated by using space-charge-limited current (SCLC).[20] As a result, improved hole injection with GraHIL increases current efficiency of OLEDs by enhancing the balance of majority carriers (i.e., electrons) and minority carriers (i.e., holes) in the EML (Figure 2b).

DOI: 10.1021/am5072628
ACS Appl. Mater. Interfaces 2015, 7, 3117−3125

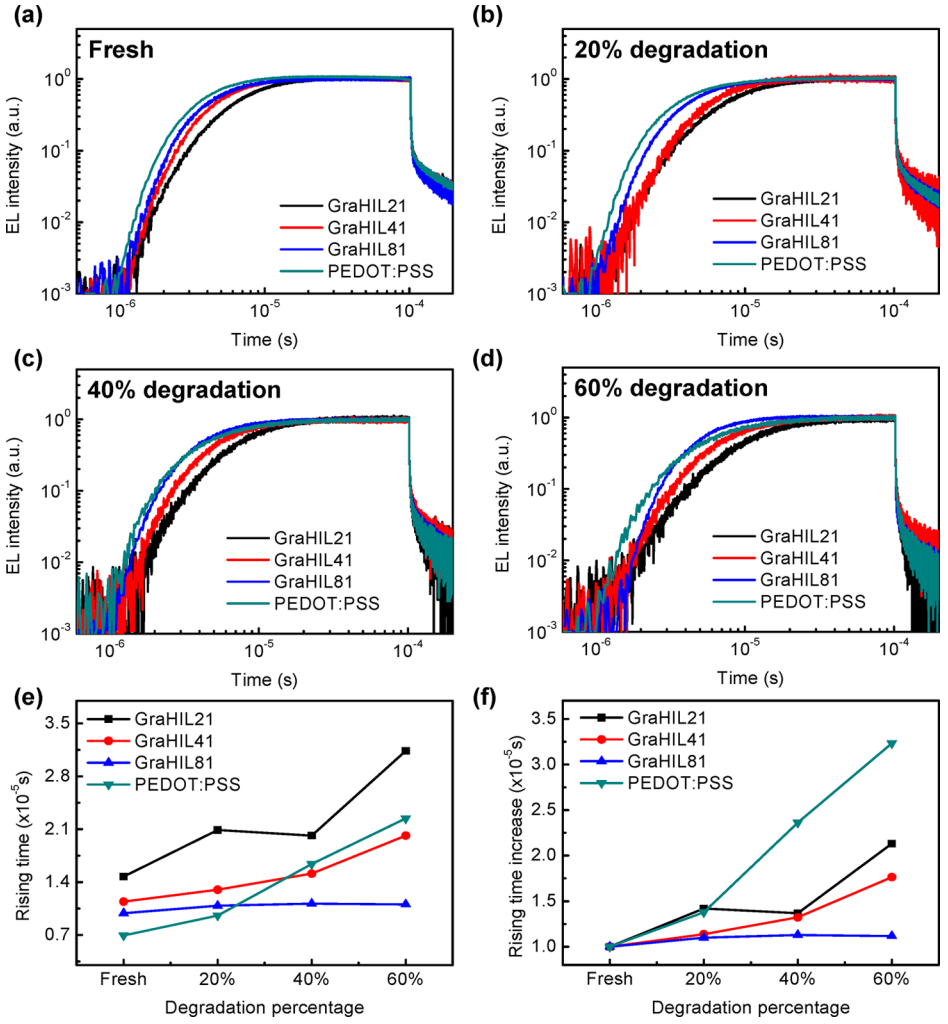

Figure 4. Transient EL measurement of OLEDs using GraHIL21, GraHIL41, GraHIL81 or PEDOT:PSS. Transient EL rising characteristics of devices at (a) fresh (0%), (b) 20%, (c) 40% and (d) 60% degraded stages of initial luminance under constant current operation. Change of (e) rising time and (f) normalized rising time defined as reaching time to 90% of saturated EL intensity of devices under device degradation.

Therefore, the peak capacitance and the voltage (V_{max}) at the peak capacitance are determined by the injection and transport of charge carriers in OLED devices. Increasing the amount of PFI relative to PEDOT:PSS increases the surface WF of the GraHIL and thus it reduces the hole-injection energy barrier so that increasing the PFI content shifted peak capacitance and V_{max} to lower values at the same time (Figure 3a). As the devices degraded, the normalized peak capacitances of all devices are gradually decreased with similar tendency on all stages of degradation (Figure 3e). Although the V_{max} also exhibited a gradual shift toward higher voltage in all devices, this shift was slower in the devices with GraHILs than in the device with PEDOT:PSS (Figure 3f). The gradual reduction of peak capacitance indicates reduced accumulation of major carriers (or electrons) in the device because electron injection and transport become gradually less effective. In contrast, degradation of hole injection in the devices differed according to the kind of HILs used, because the shift of V_{max} toward higher voltage means electron−hole recombination at higher voltages due to delayed arrival of the holes at the EML. Therefore, the C−V characterizations of the devices imply that degradation of hole injection is influenced by PFI concentration in the HILs whereas degradation of electron injection is independent of HIL compositions. Consequently, a relatively rapid increase of V_{max} in the OLED with a PEDOT:PSS HIL means that its hole-injection and -transporting capability were reduced more than in OLEDs with GraHILs as the devices degraded.

Transient Electroluminescence. To confirm that PFI concentration in GraHIL compositions influences the change in hole-injection capability during device degradation, we also performed transient EL measurements (Figure 4). The saturation time of EL signal is determined by the time required for a sufficient buildup of minority carriers at recombination zone. Therefore, transient EL rising behavior also depends directly on the charge-injection and -transport capabilities in OLEDs.[29] Improved hole injection due to addition of PFI to PEDOT:PSS causes a slight shift of the recombination zone toward the cathode. Therefore, longer traveling length of minority carriers (holes) caused devices with a GraHIL to have longer EL rising time than did devices with PEDOT:PSS. Increasing the PFI concentration in the GraHIL makes a slower rise of the EL signal compared to that in the device with a pure PEDOT:PSS, in which the increase was fastest in the nondegraded state (i.e., fresh) (Figure 4a). However, the time from onset to saturation of EL (i.e., the time required to sufficient buildup of holes at recombination zone in the EML) of the device with PEDOT:PSS showed relatively significant

DOI: 10.1021/am5072628
ACS Appl. Mater. Interfaces 2015, 7, 3117−3125

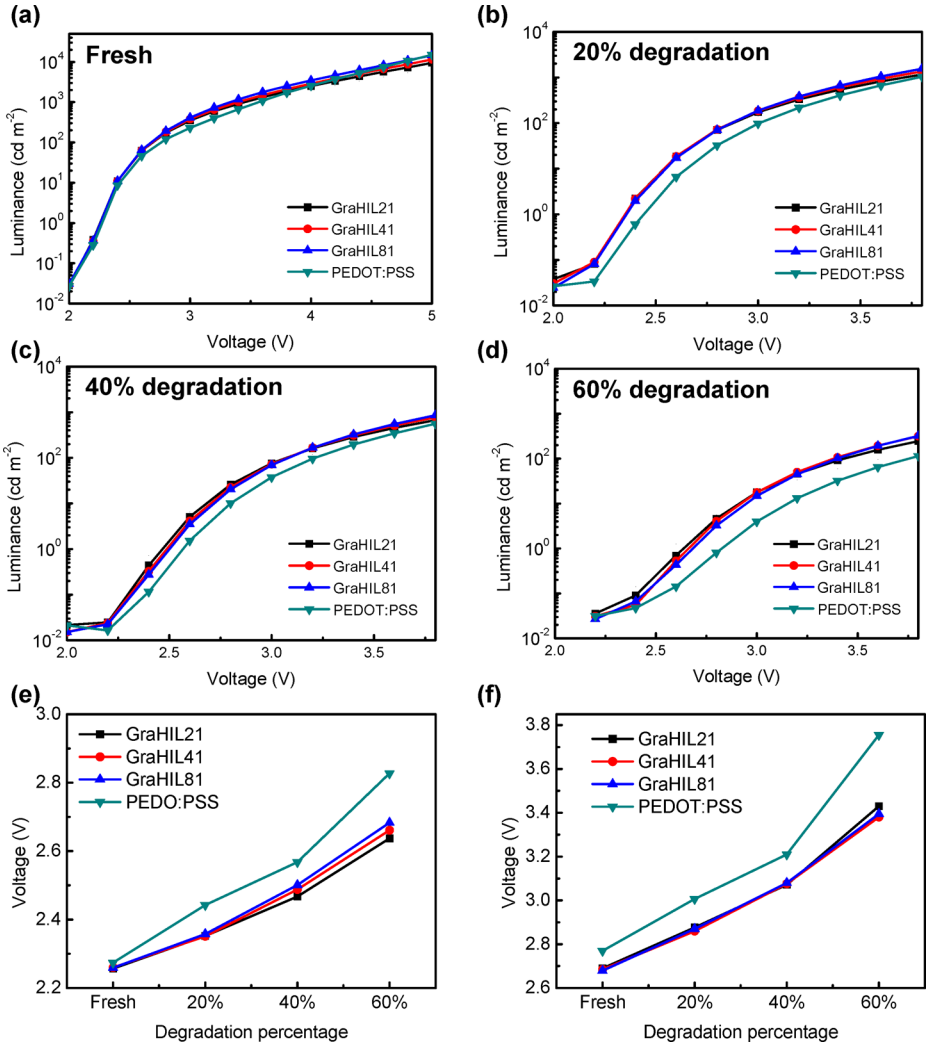

Figure 5. Luminescent characteristics of OLEDs using GraHIL21, GraHIL41, GraHIL81 or PEDOT:PSS. Luminance as a function of voltage at (a) fresh (0%), (b) 20%, (c) 40% and (d) 60% degraded stages of initial luminance under constant current operation. Change of (e) turn-on voltage (~1 cd m^{-2}) and (f) operating voltage (~100 cd m^{-2}) of devices under device degradation.

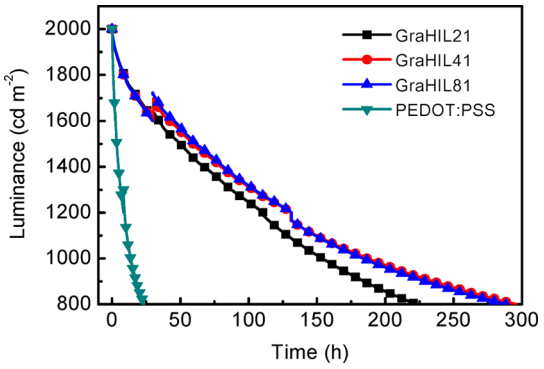

Figure 6. Operational liftimes of OLEDs using GraHIL21, GraHIL41, GraHIL81 or PEDOT:PSS.

delay during device degradation. Although the rising times (t_r) defined at 90% of saturated EL gradually increased in all devices due to reduced carrier injection and transport, the increase in t_r was much greater in the device with the PEDOT:PSS than in the devices with GraHILs (Figure 4e,f). Because both electron and hole injection/transport are gradually degraded in all the devices when the transient EL results are combined with results of C–V characterization (Figure 3), the recombination zone is expected not to change significantly under device degradation with GraHILs, judging from unshifted EL spectra (Figure 7). Because the recombination zone of PEDOT:PSS is expected to be very close to the HTL/EML interface due to large contrast of hole and electron mobilities of each layer, relatively faster degradation of hole injection/transport also cannot easily shift the recombination zone toward the anode. Therefore, transient EL results are consistent with that of C–V characteristics; together these results imply that hole injection decreased more rapidly in the device with a PEDOT:PSS than in those with GraHILs.

Current–Voltage–Luminance Characteristics. Device operation under constant current density also gradually decreased the luminescent characteristics and increased the turn-on voltage (V_{to}) (here defined as voltage at ~1 cd m^{-2}) and operating voltages of all devices (Figure 5). The rapid reduction of hole-injection ability of the PEDOT:PSS under device degradation is also demonstrated by the luminescent characteristics of the devices. Because holes injected from anode to EML through a HIL determine the electron–hole recombination at low voltage, the V_{to} may be directly related to hole injection. In the nondegraded state, V_{to} was slightly higher

DOI: 10.1021/am5072628
ACS Appl. Mater. Interfaces 2015, 7, 3117–3125

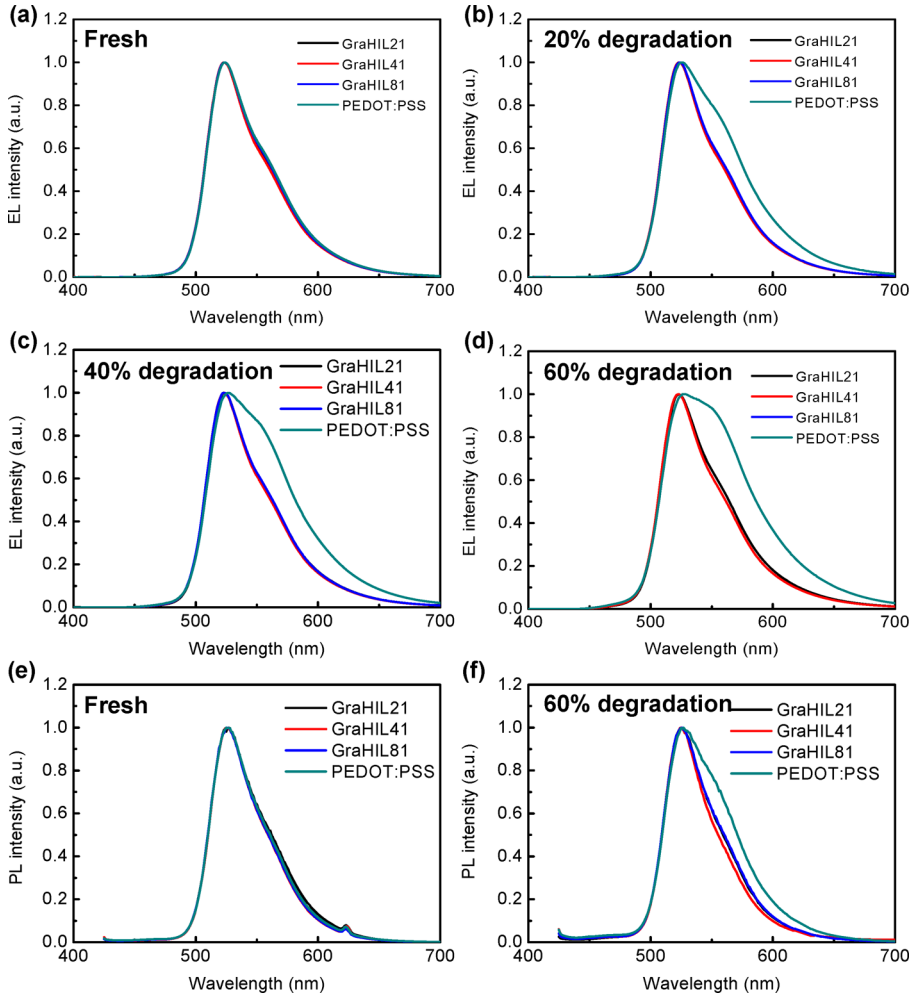

Figure 7. EL and PL characteristics of OLEDs using GraHIL21, GraHIL41, GraHIL81 or PEDOT:PSS. EL spectra of devices at (a) fresh (0%), (b) 20%, (c) 40% and (d) 60% degraded stages. PL spectra of devices at (e) fresh (0%), (f) 60% degraded stages of initial luminance under constant current operation.

in the device with a PEDOT:PSS HIL (~2.27 V) than in those with GraHILs (~2.25 V) (Figure 5a). However, device degradation rapidly increased V_{to} of the device with a PEDOT:PSS and caused a significant difference between this device (~2.83 V) and devices with GraHILs (~2.65 V) at the 60% degraded state (Figure 5e). Similarly, compared to devices with GraHILs at the same voltage, the luminance of the device with a PEDOT:PSS decreased faster and operating voltage at 100 cd m^{-2} increased faster than those with GraHILs (Figure 5f).

We tested OLED device lifetimes at constant current density that emits at about the same initial luminance (~2000 cd m^{-2}) (Figure 6). As the above-mentioned results, the luminance is more rapidly decreased in a device with PEDOT:PSS (~25 h to 40% of initial luminance) compared with those of devices with GraHILs (~300 h) at the same current density (Figure 6).

Electro- and Photoluminescence. We observed features in the EL and PL spectra of degraded devices with PEDOT:PSS that differed from those of devices using GraHILs (Figure 7). Although the normal wavelength of the maximum peak intensity is located at ~523 nm in the EL spectrum in the nondegraded stage (Figure 7a), the peak in devices using PEDOT:PSS red-shifted and broadened due to strengthening of a shoulder at ~560 nm (Figure 7b–d). The spectral change is generally contributed by shift of the recombination zone in the EML or chemical change in the emitting materials.[30,31] To determine the cause of this EL spectral change, we performed steady-state PL measurement of nondegraded and degraded devices. A similar result was observed even in the PL spectrum: nondegraded devices with all kinds of HIL had nearly identical PL spectra (Figure 7e), but in the 60% degraded devices, OLED with a PEDOT:PSS HIL showed red-shifted peak broadening in the PL spectrum, whereas those with GraHILs did not (Figure 7f). Ineffective hole injection causes accumulation not only of holes at the hole-injecting interface but also of excess electrons that do not participate in recombination with injected holes in the EML. Accumulated charges (space charges) in the organic layer can cause charged excitations such as polarons or bipolarons. These excited and unstable species can easily undergo chemical reactions with residual oxygen or moisture under device operation.[31−33] Therefore, these results imply that the emitting materials in the device with a PEDOT:PSS undergo significant chemical change during device operation; these EL and PL spectral results indicate that hole injection energy barrier and less effective hole injecion with PEDOT:PSS can cause and accelerate chemical degradation of materials in OLEDs.

DOI: 10.1021/am5072628
ACS Appl. Mater. Interfaces 2015, 7, 3117−3125

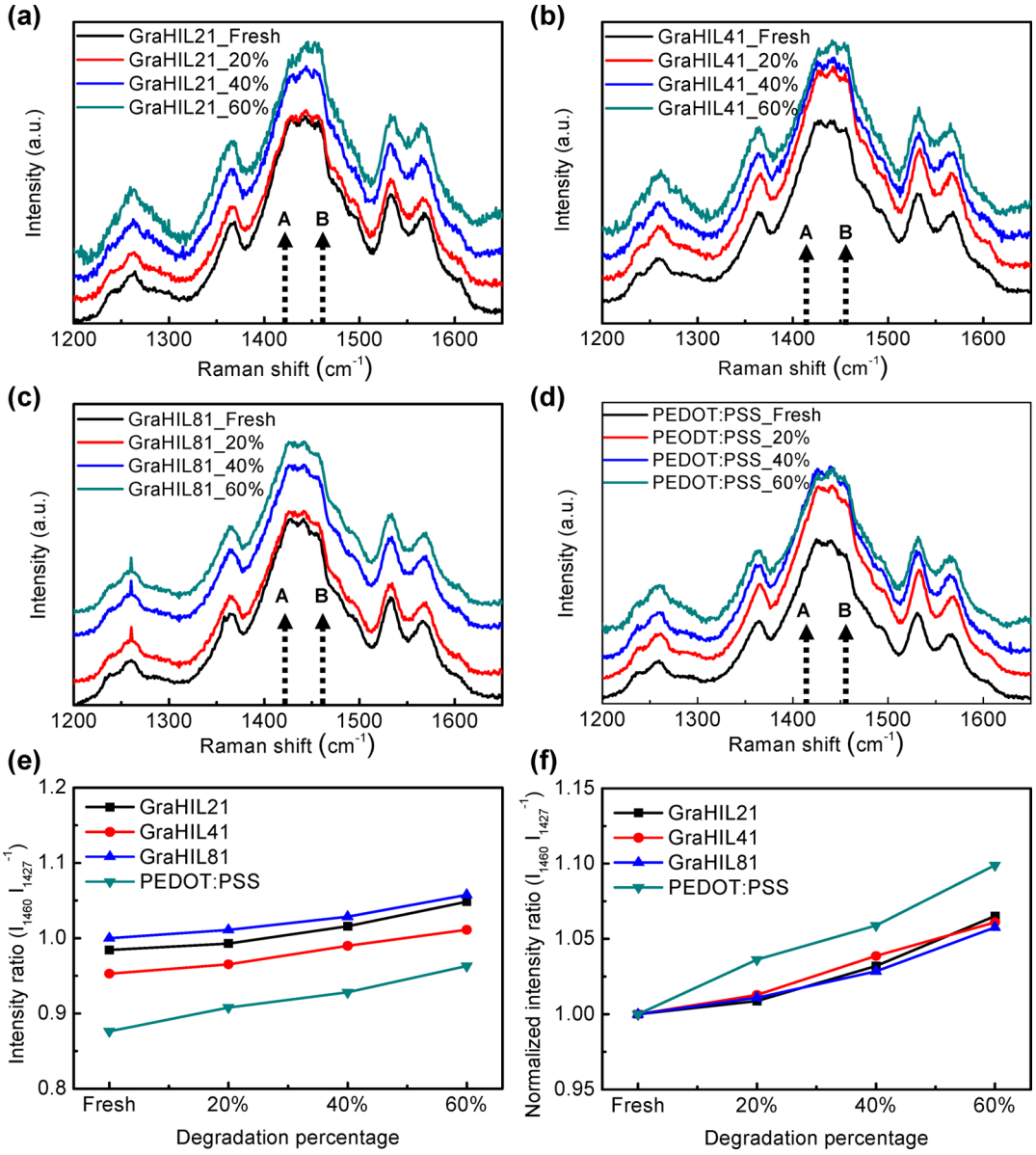

Figure 8. Results of Raman spectroscopy of OLEDs under device degradation. Raman characteristic spectra of OLEDs using (a) GraHIL21, (b) GraHIL41, (c) GraHIL81 and (d) PEDOT:PSS, (e) intensity ratio, (f) normalized intensity ratio of *B* to *A* against the degradation percentages of OLEDs (*A* ~1427 cm^{-1}; *B* ~ 1460 cm^{-1}).

Raman Spectroscopy. To investigate chemical degradation of materials in OLED devices, they were studied using Raman spectroscopy at every degradation stage. The Raman spectra revealed consistent change of the ratio (*R*) of the intensity at ~1460 cm^{-1} (*B*) to that at ~1427 cm^{-1} (*A*), which correspond to Raman bands with symmetric stretching vibrations (Figure 8).[34,35] During device degradation, *R* gradually increased in all devices and that with PEDOT:PSS exhibited a more rapid increase than those of other devices (Figure 8e,f); this change reveals that device degradation is associated with transformation of the five-membered thiophene ring in PEDOT.[34,35] As a device degrades under constant current density, the resonant structure of the PEDOT chain gradually changes from quinoid to benzoid structure,[34] which means the PEDOT changes from linear to coiled structure.[35] Coiling of PEDOT:PSS chains can interrupt interchain interaction between conducting polymer chains, so constant device operation can decrease the conductivity of the HIL.[35] Therefore, reduced conductivity of conducting polymer film may be one of the reason for reduced charge conduction under device degradation with PEDOT:PSS HIL.

Degradation Mechanism. The GraHILs contribute to efficient hole injection due to the WF gradient and the high surface WF of the self-organized PFI enriched layer. Efficient hole injection results in a good electrons and holes balance in the organic layers of OLED devices. In contrast, pure PEDOT:PSS has a relatively inefficient hole-injection ability that causes accumulation of electrons and space charges in the organic layers, which causes charged excitations such as polarons or bipolarons (Figure 9).[36,37] Furthermore, the GraHILs efficiently block the diffusion of In and Sn atoms etched during spin-coating of acidic polymer dispersion on top of the ITO anode. These charged excitations and metal atom impurities can form charge-trapping sites and induce non-radiative recombination such as polaron-exciton quenching.[38−40] By various characterizations, we deduced that carrier

DOI: 10.1021/am5072628
ACS Appl. Mater. Interfaces 2015, 7, 3117−3125

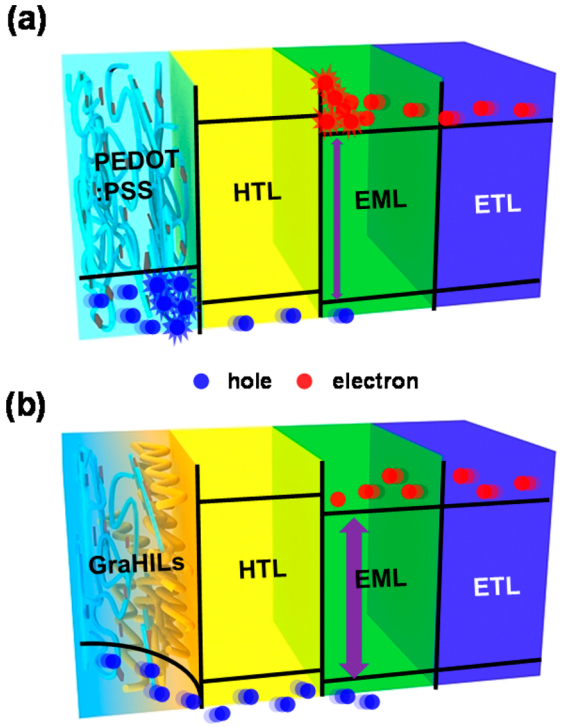

Figure 9. Schematic illustrations of operational degradation mechanism related to charge injection, transport and accumulation in OLEDs with (a) PEDOT:PSS and (b) GraHILs.

injection and transport are gradually decreased during device degradation. Because charge trapping metal impurities or charged species impede injection and transport of charges toward the emitting layer, the device degradation causes decrease in the peak capacitance, and increases in V_{max} in C−V characterization, transient EL t_r, V_{to} and operating voltage of OLEDs. All characterizations showed that these kinds of degradation were more severe in the device with a PEDOT:PSS HIL than in those with a GraHIL; the difference in severity occurs because accumulated space charges in the organic layers can accelerate the deterioration of charge injection and transport more in devices with PEDOT:PSS than in those with GraHILs. Furthermore, these charged excitations cause chemical degradation of materials; as a result, a charge imbalance due to inefficient hole injection occurs, which further aggravates charge imbalance in the EML and forms nonradiative recombination centers; therefore, the device with a PEDOT:PSS also exhibited significant drops of electro-optical performance parameters (current, luminance, and luminous efficiency) and short operational lifetime during constant current operation.

CONCLUSIONS

OLEDs fabricated using our self-organized polymeric HILs with WF gradient and high surface WF were much more efficient and stable than the device with a conventional PEDOT:PSS HIL. Device lifetime until 60% degradation under constant current density in devices with GraHILs (~300 h) was more than 10 times longer than that in the device with a with PEDOT:PSS HIL (~25 h). We studied how device stability and degradation characteristics depended on the energy barrier to hole injection by using devices with GraHILs with a range of PFI concentration in PEDOT:PSS. Non-destructive analysis methods at every degradation stage revealed that charge carrier injection and transport abilities are gradually deteriorated during device degradation. Especially, the device with a PEDOT:PSS HIL was degraded faster than did devices with GraHILs, due to differences in the energy barrier to hole injection. Inefficient hole injection by PEDOT:PSS causes accumulation of space charges, so charged excitation species such as polarons or bipolarons accumulate in organic layers and form charge-trapping sites or nonradiative recombination centers. Additionally, the self-organized PFI-enriched layer in the GraHIL can effectively block diffusion of In and Sn atoms released when PEDOT:PSS etches the ITO anode. These charged species and metal atom impurities act as charge-trapping sites and accelerate the degradation of carrier injection and transport properties of the device with a PEDOT:PSS HIL. Furthermore, gradual changes in the EL and PL spectra of the degraded device with a PEDOT:PSS HIL suggest that the chemical structure of the emitting materials changed during device operation. Consequently, current, luminance, luminous efficiency, and stability of the device with a PEDOT:PSS HIL were degraded drastically during operation. Reduction of the hole-injection barrier and increase in the hole-injection capability of the HIL are closely related to increase in the operational lifetime of OLEDs. Therefore, our study can guide to design of materials used in OLEDs to improve their efficiency and stability simultaneously.

ASSOCIATED CONTENT

Supporting Information

Surface work functions of GraHILs measured by ultraviolet photoelectron spectroscopy, chemical structure of perfluorinated ionomer, XPS depth profiles of GraHIL and setup for transient EL measurement. This material is available free of charge via the Internet at http://pubs.acs.org.

AUTHOR INFORMATION

Corresponding Author

*Tae-Woo Lee. Tel: 82-54-279-2151. Fax: 82-54-279-2399. E-mail: twlee@postech.ac.kr.

Author Contributions

T.-H. H. designed and conducted all experiments, characterizations, analysis of all the experimental results and prepared the paper. W. S. discussed experimental results and assisted with preparation of the paper. T.-W.L. initiated the study, designed all the experiments, analyzed all the data and prepared the paper. All authors in this paper discussed the experiments and results of the paper.

Notes

The authors declare no competing financial interest.

ACKNOWLEDGMENTS

This work was supported by the display research center program of Samsung Display Co., Ltd., and National Research Foundation of Korea (NRF) grant funded by the Korea government (MSIP) (NRF-2013R1A2A2A01068753).

REFERENCES

(1) Tang, C. W.; VanSlyke, S. A. Organic Electroluminescent Diodes. *Appl. Phys. Lett.* **1987**, *51*, 913−915.

(2) Kido, J.; Kimura, M.; Nagai, K. Multilayer White Light-Emitting Organic Electroluminescent Device. *Science* **1995**, *267*, 1332−1334.

(3) Shen, Z.; Burrows, P. E.; Bulovic, V.; Forrest, S. R.; Thompson, M. E. Three-Color, Tunable, Organic Light-Emitting Devices. *Science* **1997**, *276*, 2009−2011.

DOI: 10.1021/am5072628
ACS Appl. Mater. Interfaces 2015, 7, 3117−3125

(4) Baldo, M. A.; O' Brien, D. F.; Tou, Y.; Shoustikov, A.; Sibley, S.; Thomson, M. E.; Forrest, S. R. Highly Efficient Phosphorescent Emission from Organic Electroluminescent Devices. *Nature* **1998**, *395*, 151−154.
(5) Forrest, S. R. The Path to Ubiquitous and Low-Cost Organic Electronic Appliances on Plastic. *Nature* **2004**, *428*, 911−918.
(6) Reineke, S.; Lindner, F.; Schwartz, G.; Seidler, N.; Walzer, K.; Lussem, B.; Leo, K. White Organic Light-Emitting Diodes with Fluorescent Tube Efficiency. *Nature* **2009**, *459*, 234−238.
(7) Lee, J.-L.; Hong, K. Review Paper: Recent Developments in Light Extraction Technologies of Organic Light Emitting Diodes. *Electron. Mater. Lett.* **2011**, *7*, 77−91.
(8) Lee, S. J.; Koo, J. R.; Lee, S. E.; Yang, H. J.; Yoon, S. S.; Park, J.; Kim, Y. K. Effect of a Broad Recombination Zone with a Triple-Emitting Layer on the Efficiency of Blue Phosphorescent Organic Light-Emitting Diodes. *Electron. Mater. Lett.* **2014**, *10*, 1127−1131.
(9) Burrows, P. E.; Bulovic, V.; Forrest, S. R.; Sapochak, L. S.; McCarty, D. M.; Thomson, M. E. Reliability and Degradation of Organic Light Emitting Devices. *Appl. Phys. Lett.* **1994**, *65*, 2922−2924.
(10) Aziz, H.; Popovic, Z. D.; Hu, N.-X.; Hor, A.-M.; Xu, G. Degradation Mechanism of Small Molecule-based Organic Light-Emitting Devices. *Science* **1999**, *283*, 1900−1902.
(11) So, F.; Kondakov, D. Degradation Mechanisms in Small-Molecule and Polymer Organic Light-Emitting Diodes. *Adv. Mater.* **2010**, *22*, 3762−3777.
(12) D'Andrade, W.; Thompson, M. E.; Forrest, S. R. Controlling Exciton Diffusion in Multilayer White Phosphorescent Organic Light Emitting Devices. *Adv. Mater.* **2002**, *14*, 147−151.
(13) D'Andrade, B. W.; Forrest, S. R. White Organic Light-Emitting Devices for Solid-State Lighting. *Adv. Mater.* **2004**, *16*, 1585−1595.
(14) Kido, J.; Matsumoto, T. Bright Organic Electroluminescent Devices Having a Metal-Doped Electron-Injecting Layer. *Appl. Phys. Lett.* **1998**, *73*, 2866−2868.
(15) Zhou, X.; Pfeiffer, M.; Blochwitz, J.; Werner, A.; Nollau, A.; Fritz, T.; Leo, K. Very-Low-Operating-Voltage Organic Light-Emitting Diodes Using a p-Doped Amorphous Hole Injection Layer. *Appl. Phys. Lett.* **2001**, *78*, 410−412.
(16) Adachi, C.; Nagai, K.; Tamoto, N. Molecular Design of Hole Transport Materials for Obtaining High Durability in Organic Electroluminescent Diodes. *Appl. Phys. Lett.* **1995**, *66*, 2679−2681.
(17) Kim, J.-S.; Friend, R. H.; Grizzi, I.; Burroughes, J. H. Spin-Cast Thin Semiconducting Polymer Interlayer for Improving Device Efficiency of Polymer Light-Emitting Diodes. *Appl. Phys. Lett.* **2005**, *87*, 023506.
(18) Han, T.-H.; Choi, M.-R.; Woo, S.-H.; Min, S.-Y.; Lee, C.-L.; Lee, T.-W. Molecularly Controlled Interfacial Layer Strategy Toward Highly Efficient Simple-Structured Organic Light-Emitting Diodes. *Adv. Mater.* **2012**, *24*, 1487−1493.
(19) Lee, T.-W.; Chung, Y.; Kwon, O.; Park, J.-J. Self-Organized Gradient Hole Injection to Improve the Performance of Polymer Electroluminescent Devices. *Adv. Funct. Mater.* **2007**, *17*, 390−396.
(20) Choi, M.-R.; Han, T.-H.; Lim, K.-G.; Woo, S.-H.; Huh, D. H.; Lee, T.-W. Soluble Self-Doped Conducting Polymer Compositions with Tunable Work Function as Hole Injection/Extraction Layers in Organic Optoelectronics. *Angew. Chem., Int. Ed.* **2011**, *50*, 6274−6277.
(21) Han, T.-H.; Lee, Y.; Choi, M.-R.; Woo, S.-H.; Bae, S.-H.; Hong, B. H.; Ahn, J.-H.; Lee, T.-W. Extremely Efficient Flexible Organic Light-Emitting Diodes with Modified Graphene Anode. *Nat. Photonics* **2012**, *6*, 105−110.
(22) Jong, M. P. D.; IJzendoorn, L. J. V.; Voigt, M. J. A. D. Stability of the Interface between Indium-Tin-Oxide and Poly(3,4-ethylenedioxythiophene)/Poly(styrenesulfonate) in Polymer Light-Emitting Diodes. *Appl. Phys. Lett.* **2000**, *77*, 2255.
(23) Sharma, A.; Andersson, G.; Lewis, D. A. Role of Humidity on Indium and Tin Migration in Organic Photovoltaic Devices. *Phys. Chem. Chem. Phys.* **2011**, *13*, 4381−4387.
(24) Shrotriya, V.; Yang, Y. Capacitance−Voltage Characterization of Polymer Light-Emitting Diodes. *J. Appl. Phys.* **2005**, *97*, 054504.
(25) Brabec, C. J.; Shaheen, S. E.; Winder, C.; Sariciftci, N. S.; Denk, P. Effect of LiF/Metal Electrodes on the Performance of Plastic Solar Cells. *Appl. Phys. Lett.* **2002**, *80*, 1288−1290.
(26) Hung, L. S.; Tang, C. W.; Mason, M. G. Enhanced Electron Injection in Organic Electroluminescence Devices Using an Al/LiF Electrode. *Appl. Phys. Lett.* **1997**, *70*, 152−154.
(27) Yoon, J.; Kim, J.-J.; Lee, T.-W.; Park, O.-O. Evidence of Band Bending Observed by Electroabsorption Studies in Polymer Light Emitting Device with Ionomer/Al or LiF/Al Cathode. *Appl. Phys. Lett.* **2000**, *76*, 2152.
(28) Liao, S.-H.; Shiu, J.-R.; Liu, S.-W.; Yeh, S.-J.; Chen, Y.-H.; Chen, C.-T.; Chow, T. J.; Wu, C.-I. Hydroxynaphthyridine-Derived Group III Metal Chelates: Wide Band Gap and Deep Blue Analogues of Green Alq3 (Tris(8-hydroxyquinolate)aluminum) and Their Versatile Applications for Organic Light-Emitting Diodes. *J. Am. Chem. Soc.* **2009**, *131*, 763−777.
(29) Ruhstaller, B.; Carter, S. A.; Barth, S.; Riel, H.; Riess, W.; Scott, J. C. Transient and Steady-State Behavior of Space Charges in Multilayer Organic Light-Emitting Diodes. *J. Appl. Phys.* **2001**, *89*, 4575−4586.
(30) Lin, T.-C.; Hsiao, C.-H.; Lee, J.-H. Study of the Recombination Zone of the NPB/Alq3Mixed Layer Organic Light-Emitting Device. *Proc. SPIE* **2005**, *5937*, 59371Q.
(31) Kondakov, D. T. Direct Observation of Deep Electron Traps in Aged Organic Light Emitting Diodes. *J. Appl. Phys.* **2005**, *97*, 024503.
(32) Meerheim, R.; Scholz, S.; Olthof, S.; Schwartz, G.; Reineke, S.; Walzer, K.; Leo, K. Influence of Charge Balance and Exciton Distribution on Efficiency and Lifetime of Phosphorescent Organic Light-Emitting Devices. *J. Appl. Phys.* **2008**, *104*, 014510.
(33) Kondakov, D. Y.; Lenhart, W. C.; Nichols, W. F. Operational Degradation of Organic Light-Emitting Diodes: Mechanism and Identification of Chemical Products. *J. Appl. Phys.* **2007**, *101*, 024512.
(34) Semaltianos, N. G.; Logothetidis, S.; Hastas, N.; Perrie, W.; Romani, S.; Potter, R. J.; Dearden, G.; Watkins, K. G.; French, P.; Sharp, M. Modification of the Electrical Properties of PEDOT:PSS by the Incorporation of ZnO Nanoparticles Synthesized by Laser Ablation. *Chem. Phys. Lett.* **2010**, *484*, 283−289.
(35) Ouyang, J.; Xu, Q.; Chu, C.-W.; Yang, Y.; Li, G.; Shinar, J. On the Mechanism of Conductivity Enhancement in Poly(3,4-ethylenedioxythiophene):Poly(styrene sulfonate) Film through Solvent Treatment. *Polymer* **2004**, *45*, 8443−8450.
(36) Dyrekelv, P.; Inganas, O.; Paloheimo, J.; Stubb, H. Photoluminescence Quenching in a Polymer Thin-Film Field-Effect Luministor. *J. Appl. Phys.* **1992**, *71*, 2816−2820.
(37) Baldo, M. A.; Forrest, S. R. Interface-Limited Injection in Amorphous Organic Semiconductors. *Phys. Rev. B* **2001**, *64*, 085201.
(38) Kondakov, D. Y.; Sandifer, J. R.; Tang, C. W.; Young, R. H. Nonradiative Recombination Centers and Electrical Aging of Organic Light-Emitting Diodes: Direct Connection between Accumulation of Trapped Charge and Luminance Loss. *J. Appl. Phys.* **2003**, *93*, 1108−1119.
(39) Popovic, Z. D.; Aziz, H. Reliability and Degradation of Small Molecule-based Organic Light-Emitting Devices (OLEDs). *IEEE J. Quantum Electron.* **2002**, *8*, 362−371.
(40) Garter, C.; Karnutsch, C.; Lemmer, U.; Pflumm, C. The Influence of Annihilation Processes on the Threshold Current Density of Organic Laser Diodes. *J. Appl. Phys.* **2007**, *101*, 023107.

DOI: 10.1021/am5072628
ACS Appl. Mater. Interfaces 2015, 7, 3117−3125